

Published in final edited form as:

Mol Psychiatry. 2014 January ; 19(1): . doi:10.1038/mp.2013.152.

Altered parvalbumin basket cell inputs in the dorsolateral prefrontal cortex of schizophrenia subjects

JR Glasier^{#1}, KN Fish^{#1}, and DA Lewis^{1,2}

¹Department of Psychiatry, University of Pittsburgh School of Medicine, Pittsburgh, PA, USA

²Department of Neuroscience, University of Pittsburgh, Pittsburgh, PA, USA

These authors contributed equally to this work.

Abstract

Cortical circuitry dysfunction in schizophrenia has been studied at many different levels of resolution, but not at the most basic unit of network organization—synaptic inputs. Multi-label electron or confocal light microscopy is required to examine specific types of synaptic inputs, and application of these methods to quantitatively study disease-related changes in human postmortem tissue has not been feasible for technical reasons. We recently developed a multi-label confocal light microscopic approach that makes possible the systematic identification and quantification of synaptic inputs, and of the relative levels of proteins localized to these inputs, in human postmortem tissue. We applied this approach to quantify parvalbumin basket cell (PVBC) inputs in area 9 of the dorsolateral prefrontal cortex from schizophrenia and matched comparison subjects. Tissue sections were triple-labeled for the 65 kD isoform of glutamic acid decarboxylase (GAD65), PV and the GABA_A receptor $\alpha 1$ subunit. PVBC axonal boutons were defined as PV/GAD65 dual-labeled puncta, and PVBC inputs were defined as a PVBC bouton that overlapped a GABA_A receptor $\alpha 1$ subunit punctum. The density of PVBC inputs was unchanged in subjects with schizophrenia, but levels of PV protein were lower in PVBC boutons. In concert with prior reports, these findings indicate that PVBC dysfunction in schizophrenia reflects molecular and not structural alterations in these cells and their axon terminals.

Keywords

chandelier cell; GABA_A receptor; gamma oscillations; glutamic acid decarboxylase; pyramidal neuron; quantitative microscopy

Schizophrenia is a complex disorder lacking an effective treatment option for the pervasive and debilitating cognitive impairments experienced by patients.¹ Working memory, a core cognitive process impaired in schizophrenia, depends upon proper activation of circuitry in the dorsolateral prefrontal cortex (DLPFC).^{2,3} One cortical process thought to be essential for working memory is fast, synchronized neuronal activity in the gamma frequency (30–80 Hz).^{4–6} Accordingly, individuals diagnosed with schizophrenia show altered DLPFC activation during tasks that involve working memory,⁷ including lower power of prefrontal gamma oscillations.^{8,9}

© 2013 Macmillan Publishers Limited All rights reserved

Correspondence: Dr DA Lewis, Department of Psychiatry, Western Psychiatric Institute and Clinic, University of Pittsburgh, Biomedical Science Tower, Room W1651, Pittsburgh, PA 15213, USA. lewisda@upmc.edu.

CONFLICT OF INTEREST

Drs Glasier and Fish have no conflict of interest.

Gamma oscillations require the strong, synchronous inhibition of excitatory pyramidal cells by parvalbumin basket cells (PVBCs).¹⁰ PVBCs robustly innervate the soma and proximal dendrites and spines of pyramidal cells,¹¹ and their activity is strongly coupled to the gamma rhythm.^{12–14} Indeed, increasing excitation of PV neurons induces gamma oscillations,^{15,16} whereas decreasing excitatory drive to PV neurons impairs gamma oscillations and working memory performance in mice.¹⁷ Unlike PVBCs, PV chandelier cells likely do not participate in gamma oscillation generation.^{12,18,19} Thus, alterations specifically within PVBC connectivity could underlie impaired gamma oscillations and working memory performance in schizophrenia subjects.

A number of deficits in PV neurons have been identified in the DLPFC of subjects with schizophrenia (reviewed in Lewis *et al.*²⁰). In layers 3–4, the primary location of PV neurons,²¹ PV mRNA is ~30% lower,²² and the density of PV-immunoreactive puncta (small structures that could include the axon terminals of PVBC or thalamic projections) is ~20% lower in schizophrenia subjects.²³ Notably, these deficits are not accompanied by a change in PV neuron density, as both mRNA and protein studies have shown no difference in the density of DLPFC PV-positive neurons between healthy comparison and schizophrenia subjects.^{22,24,25} GABA synthesis also appears to be altered in PV neurons. Expression of mRNA for the 67 kD isoform of glutamic acid decarboxylase (GAD67), one of two GABA synthesizing enzymes, is undetectable in ~50% of PV neurons²² in subjects with schizophrenia, and GAD67 protein levels are ~50% lower in PV-immunoreactive axon terminals.²⁶ Synapses formed by PVBCs are particularly enriched with GABA_A receptors that contain $\alpha 1$ subunits,^{27,28} and some, but not all,²⁹ postmortem studies have demonstrated lower GABA_A receptor $\alpha 1$ subunit mRNA expression in the DLPFC at the tissue, laminar and cellular levels.^{30–34} For example, GABA_A receptor $\alpha 1$ subunit mRNA expression is ~40% lower in layer deep 3 pyramidal cells.³¹ Together these results suggest that in schizophrenia both the pre- and postsynaptic components of PVBC inputs to pyramidal neurons are affected such that the density and/or strength of PVBC inputs to pyramidal cells is decreased in DLPFC layer deep 3.

To test this hypothesis, we used a recently developed approach³⁵ that permits the identification and quantification of neuronal inputs, and of the levels of proteins localized to these inputs, within human postmortem tissue using the following: (1) triple immunofluorescence labeling of pre- and postsynaptic proteins; (2) a fourth measure to exclude the confounding effects of lipofuscin autofluorescence in human neocortex; (3) systematic sampling and spinning disk confocal microscopy imaging; (4) custom threshold/morphological segmentation algorithms; and (5) the three-dimensional relationship between each label. This approach permits, for the first time, quantitative assessments of the integrity of a specific type of neuronal connection in schizophrenia.

MATERIALS AND METHODS

Subjects

Brain specimens from 20 subjects were recovered during autopsies conducted at the Allegheny County Medical Examiner's Office (Pittsburgh, PA, USA) after obtaining consent from the next of kin. An independent committee of experienced research clinicians made consensus DSM-IV diagnoses for each subject using the results of structured interviews conducted with family members and review of medical records, as previously described.^{22,26} To control experimental variance and reduce biological variance between groups, each schizophrenia subject ($n = 10$) was matched for sex (seven men and three women), and as closely as possible for age, with one healthy comparison subject. Healthy comparison and schizophrenia subject mean \pm s.d. values for age at time of death (50.4 ± 18.8 and 51.5 ± 17.8 years, respectively), postmortem interval (16.5 ± 5.7 and 16.9 ± 8.1 h,

respectively), brain pH (6.8 ± 0.3 and 6.8 ± 0.3 , respectively) and freezer storage time (159.5 ± 25.5 and 167.2 ± 24.8 months, respectively) did not differ (all $t < 0.5$, $df = 18$, $P > 0.5$). All procedures were approved by the University of Pittsburgh's Committee for the Oversight of Research Involving the Dead and Institutional Review Board for Biomedical Research.

Immunohistochemistry

The left hemisphere of each brain was blocked coronally at 1.0–2.0 cm intervals, fixed in cold 4% paraformaldehyde for 48 h and immersed in a series of graded sucrose solutions. Tissue blocks containing the superior frontal gyrus were sectioned coronally at $40 \mu\text{m}$ on a cryostat and stored in antifreeze solution at $-30 \text{ }^\circ\text{C}$ until processing for immunohistochemistry. Three sections per subject, each spaced $\sim 400 \mu\text{m}$ apart, were used. One section from each subject of a pair were processed together to minimize experimental variance within or across subject pairs. Sections were incubated for 48 h in the following primary antibodies: rabbit anti-PV (1:750, Swant, Bellinzona, Switzerland), goat anti-GAD65 (1:50, R&D Systems, Minneapolis, MN, USA) and mouse anti-GABA_A receptor $\alpha 1$ subunit (1:200, Millipore, Billerica, MA, USA). The specificity of the mouse anti-GABA_A receptor $\alpha 1$ subunit has been previously described.³⁶ The specificity of the goat anti-GAD65 has been shown by immunoblot in our laboratory (data not shown) and described in the R&D Systems data sheet. The specificity of the rabbit anti-PV antibody has been previously described.³⁷ Sections were then incubated for 24 h in secondary antibodies (donkey) conjugated to Alexa 488, 568 and 647 (1:500, Invitrogen, Grand Island, NY, USA). The final channel assignment was GABA_A receptor $\alpha 1$ subunit (Alexa 488), PV (Alexa 568) and GAD65 (Alexa 647). After washing, sections were mounted (Vectashield mounting media for fluorescence), coded to obscure diagnosis and subject number, and stored at $4 \text{ }^\circ\text{C}$ until imaging.

Microscopy and sampling

Image stacks (768×768 pixels; $0.25 \mu\text{m}$ Z-step) were collected on an Olympus IX71 inverted microscope (Center Valley, PA, USA) equipped with an Olympus DSU spinning disk, using a 60XSC 1.42 N.A. oil immersion objective. The spinning disk confocal microscope was equipped with a Hamamatsu 1394 ORCA camera (Bridgewater, NJ, USA) and high precision BioPrecision2 motorized stage with linear XYZ encoders (Ludl Electronic Products, Hawthorne, NY, USA), and controlled by SlideBook 5.0 (Intelligent Imaging Innovations, Denver, CO, USA), the same software used for post-processing. TetraSpeck 0.1 mm microspheres (fluorescent blue/green/orange/dark red; Invitrogen) were used to confirm the absence of alignment issues between wavelengths.

All imaging occurred in layer deep 3 (where PVBCs are predominately located), defined as extending between 35 and 50% of the distance from the pial surface to the layer 6-white matter border, and was performed by one person who was blind to subject diagnosis. Sites were systematically and randomly sampled using a $200 \times 200 \mu\text{m}$ sampling grid. Running means using pilot data indicated that 10 sites per section were sufficient to adequately sample the region; thus, we collected image stacks from 15 sites within layer deep 3 of each section. Channel exposure times were optimized such that no pixels were saturated and the dynamic range of the camera was filled. The top 1/3 of each tissue section was imaged.

A potential confound of quantitative fluorescence measures in human cortex is lipofuscin autofluorescence.³⁸ To exclude this potential confound, lipofuscin was imaged using a fourth channel (equivalent to Alexa 405) at a constant exposure time across all sections. Lipofuscin autofluorescence was masked by one person blind to subject diagnosis, using a single optimal threshold value for each image stack. All PV, GAD65 and GABA_A receptor

$\alpha 1$ subunit masks that overlapped a lipofuscin mask, or contained fluorescent signal in the 405 channel 115 arbitrary units (a.u.), were eliminated from the analysis (Figure 1).

Image processing

Image stacks were normalized for exposure time in each channel, cropped to $39 \times 39 \mu\text{m}$ and the top 10% of Z-planes were eliminated because of the irregularities in the tissue surface associated with cryostat-cut sections. Thus, on average, 53 ± 7 Z-planes for each sampling site were analyzed. Image Z-stacks were then deconvolved using the AutoQuant adaptive blind deconvolution algorithm to improve the clarity of the data by improving resolving power, removing out-of-focus haze and eliminating noise.

A custom threshold/morphological segmentation algorithm was used to create object masks of immunoreactive puncta, identified as small ($0.03\text{--}0.7 \mu\text{m}^3$), distinct fluorescing objects, representing labeled pre- or postsynaptic structures. This segmentation algorithm used the Ridler-Calvard iterative thresholding method³⁹ to obtain an initial value for iterative segmentation. The Ridler-Calvard method chooses an initial threshold based on the assumption that the histogram for each channel is the sum of the distributions for both signal and background pixels, and then iteratively calculates a new threshold by taking the mean of the average intensities of the signal and background pixels determined by the initial threshold. This process is repeated until the threshold converges. For optimal masking of pre- and postsynaptic structures, 100 iterations with subsequent threshold settings increasing by 50 gray levels were performed.

Definitions of synaptic structures

Mask operations in SlideBook were used to identify PVBC inputs. Labeling for GAD65, which is preferentially targeted to boutons,⁴⁰ was used to classify immunoreactive puncta as GABAergic boutons. A PV-GABAergic bouton was defined as a PV object mask that contained the center of a GAD65 object mask, and a PVBC input was defined as a PV-GABAergic bouton that overlapped a GABA_A receptor $\alpha 1$ subunit object mask (Figure 2). Importantly, glutamatergic PV axonal boutons from the thalamus were excluded by using GAD65 to identify boutons. As PV chandelier cells do not contain GAD65 in non-human primate PFC³⁵ and because their inputs are not enriched with $\alpha 1$ -containing GABA_A receptors,⁴¹ our approach excluded PV chandelier cell boutons. Several important aspects of the experimental and classification design mitigate the limitations of using light microscopy to identify synapses: (1) the use of two presynaptic markers (PV and GAD65) and a postsynaptic marker (GABA_A $\alpha 1$ subunit), (2) strict object mask size requirements that were restricted to a biologically relevant range for pre- and postsynaptic structures and (3) strict spatial relationship criteria among the three markers.

Statistics

An analysis of covariance model was performed on each dependent measure using diagnostic group as the main effect and sex, age, race, postmortem interval, pH and storage time as covariates. The only covariate that significantly affected any dependent measure was an effect of postmortem interval on PVBC input density ($F_{(1, 12)}=6.186$, $P=0.029$).

RESULTS

GAD65 is expressed in PVBC boutons but not in PV chandelier cell boutons

We have previously shown in non-human primate DLPFC that PV chandelier cell boutons exclusively express GAD67, whereas PVBCs express both GAD65 and GAD67.³⁵ We performed the same analysis in three healthy comparison subjects to determine whether this

relationship was conserved in human DLPFC (Figure 3). Indeed, mean GAD65 fluorescence intensity was 99% lower ($t_{(4)}=12.5$, $P<0.001$) in PV chandelier boutons (11.3 ± 2.5 a.u.) relative to PVBC boutons ($1\ 206.7\pm 165.7$ a.u.). Mean GAD67 fluorescence intensity did not differ ($t_{(4)}=1.8$, $P=0.15$) between PV chandelier boutons (971.8 ± 162.2 a.u.) and PVBC boutons ($1\ 207.3\pm 164.5$ a.u.). Thus, as in monkey DLPFC, PVBC boutons in human DLPFC contain both GAD65 and GAD67.

PVBC input density is unchanged in schizophrenia

A total of 63 621 and 71 359 triple-labeled PVBC inputs were analyzed in the 10 pairs of comparison and schizophrenia subjects, respectively. The mean density of PVBC inputs did not differ ($F_{(1, 12)}=2.126$, $P=0.17$) between healthy comparison ($12.5/\text{mm}^3\pm 2.2$) and schizophrenia ($14.1/\text{mm}^3\pm 2.4$) subjects (Figure 4a). These data demonstrate that schizophrenia is not associated with a loss of DLPFC PVBC inputs.

Relative PV protein levels are lower in PVBC inputs in schizophrenia

We next quantified GAD65, PV and GABA_A receptor $\alpha 1$ subunit fluorescence intensities within PVBC inputs to assess measures that may affect PVBC synaptic strength.

Mean PV fluorescence intensity was 23% lower (Figure 4b; $F_{(1, 12)}=7.531$, $P=0.018$) in PVBC boutons of schizophrenia subjects ($4\ 794.2$ a.u. ± 993.7) relative to healthy comparison subjects ($6\ 212.3$ a.u. ± 1397.1). GAD65 and GABA_A $\alpha 1$ mean fluorescence intensities did not differ (Figure 4b; all $F_{(1, 12)}<0.87$, $P>0.36$) between healthy comparison and schizophrenia subjects.

DISCUSSION

To date, methodological obstacles have precluded the quantification of disease-related effects on synaptic inputs from an identified neuronal population in human postmortem tissue. Using an approach recently developed in our laboratory, we conducted the first quantitative examination of PVBC inputs in schizophrenia subjects. Our findings demonstrate that the density of PVBC inputs in the DLPFC is unchanged in schizophrenia, but that PVBC axonal bouton levels of PV protein are lower. These findings are supported by previous studies showing no deficit in PV cell number but lower PV mRNA expression per neuron in the DLPFC of schizophrenia subjects (reviewed in Lewis *et al.*²⁰). The current findings also clarify the interpretation of a single-label immunoperoxidase study, which found a lower density of PV-immunoreactive puncta, presumed axonal boutons, in the middle layers of DLPFC area 9 in schizophrenia subjects.²³ This observation has been interpreted as possibly reflecting fewer PV-containing projections from the mediodorsal thalamic nucleus²³ and/or fewer PVBC boutons in the DLPFC of schizophrenia subjects.²⁰ However, the results of this study show that this finding likely reflects the reduction in PV protein within PVBCs to levels below those detectable by traditional immunoperoxidase methods.⁴² Thus, in concert with prior studies, our findings strongly suggest that neither the number nor axonal morphology of PVBCs are altered in schizophrenia, but that reduced PV mRNA expression results in lower levels of PV protein within PVBC axon terminals.

Prior studies have also reported lower GAD67 mRNA in PV cells²² and lower GAD67 protein in putative PVBC boutons,²⁶ suggesting that PVBC inputs have lower levels of both PV and GAD67 proteins. Whether GAD67 is lower in the PVBC inputs examined in the present study could not be determined. However, taken together, the available data suggest that GABA synthesis and calcium buffering within PVBC axon terminals is significantly lower in schizophrenia. This combination of lower protein levels with preserved PVBC

synaptic density has important implications for determining whether these alterations might reflect a cause or consequence of DLPFC dysfunction in schizophrenia.

The combination of a normal density of PVBC inputs and lower PV and GAD67²⁶ protein levels per bouton, but no compensatory upregulation of GAD65 or postsynaptic $\alpha 1$ -containing GABA_A receptors, could reflect either of two possible upstream events. Schizophrenia is thought to be a disorder of neurodevelopment, and incomplete maturation of PVBCs may be the underlying cause of lower PV and GAD67. For example, although the number of PVBC inputs reaches adult levels by 3 months of age in monkey DLPFC, the amount of PV in these inputs increases substantially from the perinatal period through late adolescence.^{43,44} Thus, our current findings of a normal density of PVBC inputs but lower levels of PV protein per bouton could reflect a developmental disturbance that occurs after PVBC synapses are established, but before PV reaches adult levels in PVBCs, that is sometime between childhood and late adolescence. Interestingly, in children who will develop schizophrenia later in life, working memory performance appears normal at age seven, and then lags behind the normal rate of improvement.^{45–47} Future confirmation of this time course for the appearance of PVBC disturbances would represent a unique opportunity to utilize preemptive strategies that normalize PVBC maturation.

Alternatively, these findings could reflect molecular consequences of chronic reductions in excitatory drive to layer 3 DLPFC pyramidal cells in schizophrenia.²⁰ For example, PV⁴⁸ and GAD67⁴⁹ expression is activity dependent, and PVBCs receive dense excitatory innervation from layer 3 pyramidal cells.⁵⁰ DLPFC layer 3 pyramidal cells exhibit several alterations suggestive of decreased excitation in schizophrenia, such as lower dendritic spine density.⁵¹ Together, these data suggest that lower excitation and activity of layer 3 pyramidal cells may preferentially reduce PVBC activation, leading to a downregulation of PV and GAD67 expression.

Whether a cause or consequence, the current findings help to focus the search for appropriate pharmacological targets to ameliorate DLPFC dysfunction in schizophrenia. As the number of PVBC inputs is preserved, modulating their activity represents a viable option to restore DLPFC functioning in schizophrenia as lower PV and GAD67 protein levels within PVBC boutons are likely to contribute to the reduced power of prefrontal gamma oscillations in schizophrenia.^{20,52} For example, a recent computational modeling study reported that decreasing both PV and GABA within PV neurons reduced stimulus-induced gamma band power in a manner similar to that observed in schizophrenia subjects.⁵² Thus, lower PV and GAD67 protein within PVBCs may represent a key substrate for impaired gamma oscillations and working memory in schizophrenia subjects, and modulating their expression and/or function within PVBCs represents a potential therapeutic strategy.

Acknowledgments

The authors gratefully acknowledge Brad Rocco for his expertise and assistance with image processing, and Wasiq Sheikh for his imaging assistance.

David A Lewis currently receives investigator-initiated research support from Bristol-Myers Squibb and Pfizer and in 2011–2013 served as a consultant in the areas of target identification and validation and new compound development to Bristol-Myers Squibb and Concert Pharmaceuticals.

REFERENCES

1. Elvevag B, Goldberg TE. Cognitive impairment in schizophrenia is the core of the disorder. *Crit Rev Neurobiol.* 2000; 14:1–21. [PubMed: 11253953]
2. Miller EK, Cohen JD. An integrative theory of prefrontal cortex function. *Annu Rev Neurosci.* 2001; 24:167–202. [PubMed: 11283309]

3. Lewis DA, Gonzalez-Burgos G. Neuroplasticity of neocortical circuits in schizophrenia. *Neuropsychopharmacol Rev.* 2008; 33:141–165.
4. Howard MW, Rizzuto DS, Caplan JB, Madsen JR, Lisman J, Aschenbrenner-Scheibe R, et al. Gamma oscillations correlate with working memory load in humans. *Cereb Cortex.* 2003; 13:1369–1374. [PubMed: 14615302]
5. Uhlhaas PJ, Pipa G, Neunschwander S, Wibral M, Singer W. A new look at gamma? High- (>60 Hz) gamma-band activity in cortical networks: function, mechanisms and impairment. *Prog Biophys Mol Biol.* 2011; 105:14–28. [PubMed: 21034768]
6. Roux F, Wibral M, Mohr HM, Singer W, Uhlhaas PJ. Gamma-band activity in human prefrontal cortex codes for the number of relevant items maintained in working memory. *J Neurosci.* 2012; 32:12411–12420. [PubMed: 22956832]
7. Minzenberg MJ, Laird AR, Thelen S, Carter CS, Glahn DC. Meta-analysis of 41 functional neuroimaging studies of executive function in schizophrenia. *Arch Gen Psychiatry.* 2009; 66:811–822. [PubMed: 19652121]
8. Minzenberg MJ, Firl AJ, Yoon JH, Gomes GC, Reinking C, Carter CS. Gamma oscillatory power is impaired during cognitive control independent of medication status in first-episode schizophrenia. *Neuropsychopharmacology.* 2010; 35:2590–2599. [PubMed: 20827271]
9. Cho RY, Konecky RO, Carter CS. Impairments in frontal cortical gamma synchrony and cognitive control in schizophrenia. *Proc Natl Acad Sci USA.* 2006; 103:19878–19883. [PubMed: 17170134]
10. Bartos M, Vida I, Jonas P. Synaptic mechanisms of synchronized gamma oscillations in inhibitory interneuron networks. *Nat Rev Neurosci.* 2007; 8:45–56. [PubMed: 17180162]
11. Melchitzky DS, Sesack SR, Lewis DA. Parvalbumin-immunoreactive axon terminals in macaque monkey and human prefrontal cortex: laminar, regional and target specificity of type I and type II synapses. *J Comp Neurol.* 1999; 408:11–22. [PubMed: 10331577]
12. Dugladze T, Schmitz D, Whittington MA, Vida I, Gloveli T. Segregation of axonal and somatic activity during fast network oscillations. *Science.* 2012; 336:1458–1461. [PubMed: 22700932]
13. Tukker JJ, Fuentealba P, Hartwich K, Somogyi P, Klausberger T. Cell type-specific tuning of hippocampal interneuron firing during gamma oscillations in vivo. *J Neurosci.* 2007; 27:8184–8189. [PubMed: 17670965]
14. Hajos N, Pálhalmi J, Mann EO, Németh B, Paulsen O, Freund TF. Spike timing of distinct types of GABAergic interneuron during hippocampal gamma oscillations in vitro. *J Neurosci.* 2004; 24:9127–9137. [PubMed: 15483131]
15. Sohal VS, Zhang F, Yizhar O, Deisseroth K. Parvalbumin neurons and gamma rhythms enhance cortical circuit performance. *Nature.* 2009; 459:698–702. [PubMed: 19396159]
16. Cardin JA, Carlén M, Meletis K, Knoblich U, Zhang F, Deisseroth K, et al. Driving fast-spiking cells induces gamma rhythm and controls sensory responses. *Nature.* 2009; 459:663–667. [PubMed: 19396156]
17. Fuchs EC, Zivkovic AR, Cunningham MO, Middleton S, Lebeau FE, Bannerman DM, et al. Recruitment of parvalbumin-positive interneurons determines hippocampal function and associated behavior. *Neuron.* 2007; 53:591–604. [PubMed: 17296559]
18. Gulyas AI, Szabó GG, Ulbert I, Holderith N, Monyer H, Erdélyi F, et al. Parvalbumin-containing fast-spiking basket cells generate the field potential oscillations induced by cholinergic receptor activation in the hippocampus. *J Neurosci.* 2010; 30:15134–15145. [PubMed: 21068319]
19. Klausberger T, Somogyi P. Neuronal diversity and temporal dynamics: the unity of hippocampal circuit operations. *Science.* 2008; 321:53–57. [PubMed: 18599766]
20. Lewis DA, Curley AA, Glausier JR, Volk DW. Cortical parvalbumin interneurons and cognitive dysfunction in schizophrenia. *Trends Neurosci.* 2012; 35:57–67. [PubMed: 22154068]
21. Conde F, Lund JS, Jacobowitz DM, Baimbridge KG, Lewis DA. Local circuit neurons immunoreactive for calretinin, calbindin D-28k or parvalbumin in monkey pre-frontal cortex: distribution and morphology. *J Comp Neurol.* 1994; 341:95–116. [PubMed: 8006226]
22. Hashimoto T, Volk DW, Eggan SM, Mirmics K, Pierri JN, Sun Z, et al. Gene expression deficits in a subclass of GABA neurons in the prefrontal cortex of subjects with schizophrenia. *J Neurosci.* 2003; 23:6315–6326. [PubMed: 12867516]

23. Lewis DA, Cruz DA, Melchitzky DS, Pierri JN. Lamina-specific deficits in parvalbumin-immunoreactive varicosities in the prefrontal cortex of subjects with schizophrenia: evidence for fewer projections from the thalamus. *Am J Psychiatry*. 2001; 158:1411–1422. [PubMed: 11532725]
24. Woo T-U, Miller JL, Lewis DA. Schizophrenia and the parvalbumin-containing class of cortical local circuit neurons. *Am J Psychiatry*. 1997; 154:1013–1015. [PubMed: 9210755]
25. Beasley CL, Zhang ZJ, Patten I, Reynolds GP. Selective deficits in prefrontal cortical GABAergic neurons in schizophrenia defined by the presence of calcium-binding proteins. *Biol Psychiatry*. 2002; 52:708–715. [PubMed: 12372661]
26. Curley AA, Arion D, Volk DW, Asafu-Adjei JK, Sampson AR, Fish KN, et al. Cortical deficits of glutamic acid decarboxylase 67 expression in schizophrenia: clinical, protein, and cell type-specific features. *Am J Psychiatry*. 2011; 168:921–929. [PubMed: 21632647]
27. Klausberger T, Roberts JD, Somogyi P. Cell type- and input-specific differences in the number and subtypes of synaptic GABA_A receptors in the hippocampus. *J Neurosci*. 2002; 22:2513–2521. [PubMed: 11923416]
28. Nyíri G, Freund TF, Somogyi P. Input-dependent synaptic targeting of α_2 subunit-containing GABA_A receptors in synapses of hippocampal pyramidal cells of the rat. *Eur J Neurosci*. 2001; 13:428–442. [PubMed: 11168550]
29. Duncan CE, Webster MJ, Rothmond DA, Bahn S, Elashoff M, Shannon Weickert C, et al. Prefrontal GABA(A) receptor alpha-subunit expression in normal postnatal human development and schizophrenia. *J Psychiatry Res*. 2010; 44:673–681.
30. Beneyto M, Abbott A, Hashimoto T, Lewis DA. Lamina-specific alterations in cortical GABA_A receptor subunit expression in schizophrenia. *Cereb Cortex*. 2011; 21:999–1011. [PubMed: 20843900]
31. Glausier JR, Lewis DA. Selective pyramidal cell reduction of GABA(A) receptor alpha1 subunit messenger RNA expression in schizophrenia. *Neuropsychopharmacology*. 2011; 36:2103–2110.
32. Hashimoto T, Bazmi HH, Mirnics K, Wu Q, Sampson AR, Lewis DA, et al. Conserved regional patterns of GABA-related transcript expression in the neocortex of subjects with schizophrenia. *Am J Psychiatry*. 2008; 165:479–489. [PubMed: 18281411]
33. Akbarian S, Huntsman MM, Kim JJ, Tafazzoli A, Potkin SG, Bunney WE Jr, et al. GABA_A receptor subunit gene expression in human prefrontal cortex: comparison of schizophrenics and controls. *Cereb Cortex*. 1995; 5:550–560. [PubMed: 8590827]
34. Hashimoto T, Arion D, Unger T, Maldonado-Avilés JG, Morris HM, Volk DW, et al. Alterations in GABA-related transcriptome in the dorsolateral prefrontal cortex of subjects with schizophrenia. *Mol Psychiatry*. 2008; 13:147–161. [PubMed: 17471287]
35. Fish KN, Sweet RA, Lewis DA. Differential distribution of proteins regulating GABA synthesis and reuptake in axon boutons of subpopulations of cortical inter-neurons. *Cereb Cortex*. 2011; 21:2450–2460. [PubMed: 21422269]
36. Benke D, Cicin-Sain A, Mertens S, Mohler H. Immunohistochemical identification of the $\alpha 1$ - and $\alpha 3$ -subunits of the GABA_A-receptor in rat brain. *J Receptor Res*. 1991; 11:407–424.
37. Schwaller B, Dick J, Dhoot G, Carroll S, Vrbova G, Nicotera P, et al. Prolonged contraction-relaxation cycle of fast-twitch muscles in parvalbumin knockout mice. *Am J Physiol*. 1999; 276:C395–C403. [PubMed: 9950767]
38. Billinton N, Knight AW. Seeing the wood through the trees: a review of techniques for distinguishing green fluorescent protein from endogenous autofluorescence. *Anal Biochem*. 2001; 291:175–197. [PubMed: 11401292]
39. Ridler TW, Calvard S. Picture thresholding using an iterative selection method, *IEEE Trans. System Man Cybernetics*. 1978; 8:630–632.
40. Kaufman DL, Houser CR, Tobin AJ. Two forms of the gamma-aminobutyric acid synthetic enzyme glutamate decarboxylase have distinct intraneuronal distributions and cofactor interactions. *J Neurochem*. 1991; 56:720–723. [PubMed: 1988566]
41. Mohler H. GABA(A) receptor diversity and pharmacology. *Cell Tissue Res*. 2006; 326:505–516. [PubMed: 16937111]

42. Fish KN, Sweet RA, Deo AJ, Lewis DA. An automated segmentation methodology for quantifying immunoreactive puncta number and fluorescence intensity in tissue sections. *Brain Res.* 2008; 1240:62–72. [PubMed: 18793619]
43. Huang HS, Matevosian A, Whittle C, Kim SY, Schumacher A, Baker SP, et al. Prefrontal dysfunction in schizophrenia involves mixed-lineage leukemia 1-regulated histone methylation at GABAergic gene promoters. *J Neurosci.* 2007; 27:11254–11262. [PubMed: 17942719]
44. Fish KN, Hoftman GD, Sheikh W, Kitchens M, Lewis DA. Parvalbumin-containing chandelier and basket cell boutons have distinctive modes of maturation in monkey prefrontal cortex. *J Neurosci.* 2013; 33:8352–8358. [PubMed: 23658174]
45. Lesh TA, Niendam TA, Minzenberg MJ, Carter CS. Cognitive control deficits in schizophrenia: mechanisms and meaning. *Neuropsychopharmacology.* 2011; 36:316–338. [PubMed: 20844478]
46. Davidson M, Reichenberg A, Rabinowitz J, Weiser M, Kaplan Z, Mark M, et al. Behavioral and intellectual markers for schizophrenia in apparently healthy male adolescents. *Am J Psychiatry.* 1999; 156:1328–1335. [PubMed: 10484941]
47. Reichenberg A, Caspi A, Harrington H, Houts R, Keefe RS, Murray RM, et al. Static and dynamic cognitive deficits in childhood preceding adult schizophrenia: a 30-year study. *Am J Psychiatry.* 2010; 167:160–169. [PubMed: 20048021]
48. Carder RK, Leclerc SS, Hendry SHC. Regulation of calcium-binding protein immunoreactivity in GABA neurons of macaque primary visual cortex. *Cereb Cortex.* 1996; 6:271–287. [PubMed: 8670656]
49. Jones EG. GABAergic neurons and their role in cortical plasticity in primates. *Cereb Cortex.* 1993; 3:361–372. [PubMed: 8260806]
50. Melchitzky DS, Lewis DA. Pyramidal neuron local axon terminals in monkey prefrontal cortex: differential targeting of subclasses of GABA neurons. *Cereb Cortex.* 2003; 13:452–460. [PubMed: 12679292]
51. Glantz LA, Lewis DA. Decreased dendritic spine density on prefrontal cortical pyramidal neurons in schizophrenia. *Arch Gen Psychiatry.* 2000; 57:65–73. [PubMed: 10632234]
52. Volman V, Behrens MM, Sejnowski TJ. Downregulation of parvalbumin at cortical GABA synapses reduces network gamma oscillatory activity. *J Neurosci.* 2011; 31:18137–18148. [PubMed: 22159125]

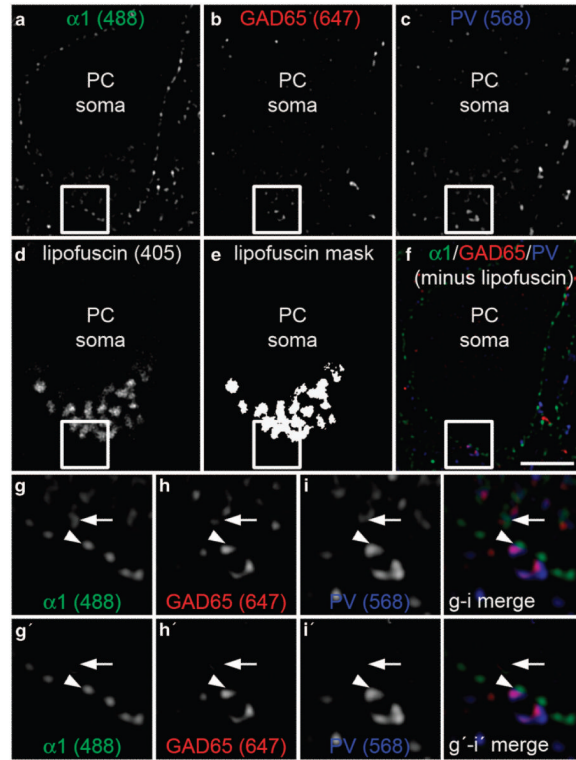


Figure 1. Four channel imaging experimental design. Sections containing human dorsolateral prefrontal cortex (DLPFC) area 9 were imaged for (a) GABA_A α 1 subunit (488 channel), (b) glutamic acid decarboxylase 65 (GAD65; 647 channel), (c) parvalbumin (PV; 568 channel) and (d) lipofuscin autofluorescence, which is visible in all channels (405 channel). (e) Mask of the lipofuscin signal. (f) Merged image of remaining immunolabel used for analysis after lipofuscin subtraction. (g–i) 3X zoom of the boxed region showing fluorescent signal in the 488, 647 and 568 channels, respectively. (g'–i') 3X zoom of the boxed region showing fluorescent signal in the 488, 647 and 568 channels, respectively, after lipofuscin autofluorescence subtraction. Filled arrowhead indicates a triple-immunolabeled parvalbumin basket cell (PVBC) input included in final analysis. Filled arrow indicates a false-positive PVBC input (g–i merge) eliminated after lipofuscin autofluorescence subtraction (g'–i' merge). Scale bar: 5 μ m. PC, pyramidal cell.

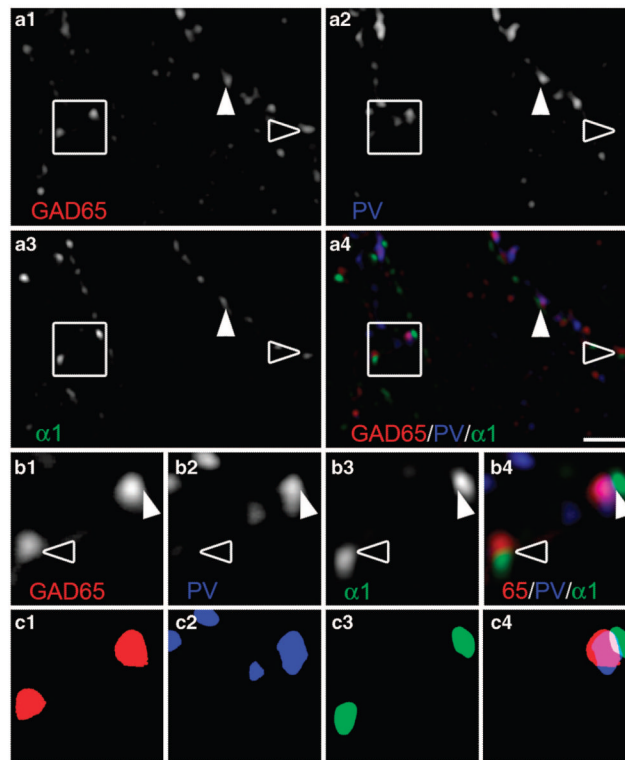


Figure 2.

Classification of GABAergic inputs. Human dorsolateral prefrontal cortex (DLPFC) multi-labeled for glutamic acid decarboxylase 65 (GAD65), parvalbumin (PV) and the GABA_A α 1 subunit. **(a1–a3)** Single channel and **(a4)** merged images. **(b1–b4)** 3X zoom of the boxed region in **a1–a4**. **(c1–c3)** Object masks of immunoreactive puncta in **b1–b3**. **(c4)** Overlapping object masks marking the parvalbumin basket cell (PVBC) input in **b4**. In each panel, filled arrowheads indicate PVBC inputs; open arrowheads indicate PV-negative GABAergic inputs, which were excluded from analyses. Scale bar: 2 μ m.

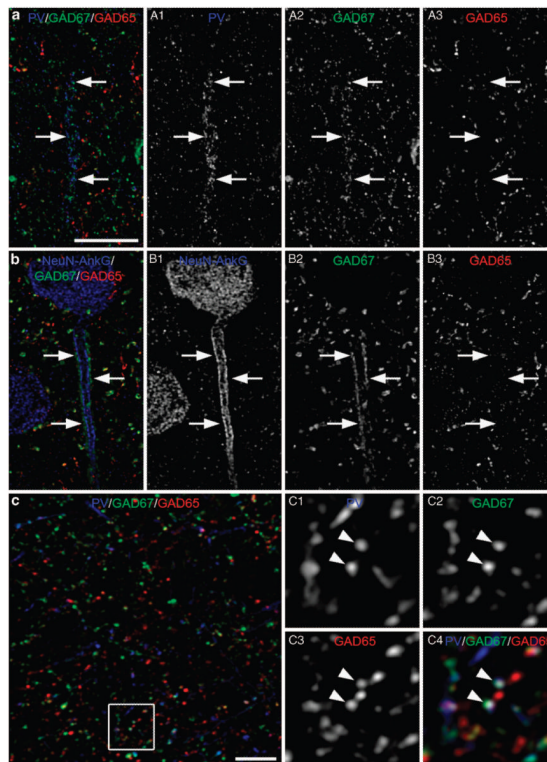


Figure 3.

Glutamic acid decarboxylase 65 (GAD65) colocalizes with parvalbumin basket cell (PVBC) boutons and not parvalbumin (PV) chandelier cartridges. **(a)** Merged image of human dorsolateral prefrontal cortex (DLPFC) labeled for PV, GAD67 and GAD65 showing a PV chandelier cell axon cartridge delineated by filled arrows. (A1–A3) Single channel images of panel **a** illustrating an abundance of PV and GAD67, with an absence of GAD65, in the cartridge. **(b)** Merged image of human DLPFC labeled for NeuN and Ankyrin-G (AnkG) to label pyramidal cell somata and axon initial segments (AIS), respectively, GAD67 and GAD65. The AIS, which is delineated by filled arrows, is heavily innervated by GAD67-positive boutons, but lacks innervation by GAD65-positive boutons. (B1–B3) Single channel images of panel **b**. **(c)** Merged image of human DLPFC labeled for PV, GAD67 and GAD65 in a region lacking PV chandelier cell axon cartridges. (C1–C4) 3X zoom of the boxed region in panel **c** showing single channel images for PV, GAD67 and GAD65. Filled arrowheads indicate triple-labeled PV axonal boutons. Scale bar in panel **a** is also for panel **b**, scale bar: 10 μm .

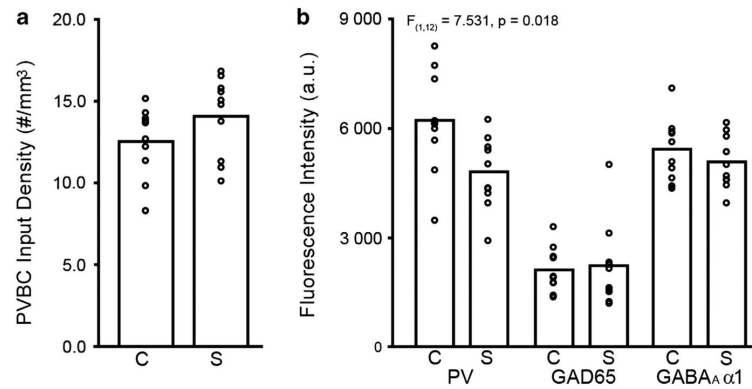


Figure 4.

Density and fluorescence intensities of parvalbumin basket cell (PVBC) inputs in schizophrenia (S) and healthy comparison (C) subjects. Bars indicate mean values for a diagnostic group, and open circles represent mean values for individual subjects. **(a)** Mean PVBC input density did not differ between groups. **(b)** Mean parvalbumin (PV) fluorescence intensity per PVBC bouton was significantly lower in schizophrenia subjects relative to healthy comparison subjects, but fluorescence intensity measures for GAD65 and GABA_A receptor α1 subunit did not differ between groups. a.u., arbitrary unit.